

# The influence of sample thickness on the tensile properties of pure Cu with different grain sizes

L. Yang and L. Lu\*

Shenyang National Laboratory for Materials Science, Institute of Metal Research, Chinese Academy of Sciences,  
72 Wenhua Road, Shenyang 110016, People's Republic of China

Received 26 March 2013; revised 5 April 2013; accepted 5 April 2013  
Available online 12 April 2013

We investigate the effects of sample thickness on the tensile properties of pure Cu with different grain sizes. Tensile strength, ductility and work-hardening coefficient decrease with decreasing sample thickness when the  $t/d$  (sample thickness/average grain size) is smaller than a critical value. It is suggested that the thickness effects are governed by competition between the dislocation activities in the interior grains and surface grains.

© 2013 Acta Materialia Inc. Published by Elsevier Ltd. All rights reserved.

**Keywords:** Sample thickness effect; Cu; Tensile strength; Ductility; Deformation mechanism

The mechanical properties of polycrystalline metallic materials are not only dominated by intrinsic microstructural features, such as the grain size dependence as described by the well-known Hall–Petch relationship [1–2], but are also closely related to certain extrinsic conditions, such as strain rate [3–4], temperature [5], as well as sample size geometry itself. In order to eliminate the effect of sample geometry on the mechanical properties, the geometry of specimens being studied should meet the American Society for Testing and Materials (ASTM) standard [6]. However, sometimes sample sizes cannot fit the ASTM standard, and non-standard miniature dog-bone tensile specimens with different thicknesses and geometries are frequently used in the literature to explore the tensile behavior, especially for samples with nanometer or submicron-sized grains where the geometric size limitations of the samples were generally caused by the challenge of preparation techniques [7–9].

A previous survey of the literature results by Miyazaki et al. indicated that the flow stress decreased with decreasing specimen thickness when the ratio of the specimen thickness to grain size was smaller than a critical value [10]. They considered that the affected zone around the deformed grain dominated the sample size effects. The effect of surface grains was investigated by Fulop et al. [11] via computational simulations. The

“surface layer model” states that the surface grains are less hard compared to the interior ones, while the share of this surface grain increases with a decrease in specimen size [12]. Zhao et al. [13] reported a significant influence of specimen dimension on the tensile behavior of ultrafine-grained Cu prepared by means of equal-channel angular pressing (ECAP), where the elongation to failure, post-necking elongation and strain-hardening rate all increase with increasing thickness or decreasing gauge length. However, strain softening generally occurred shortly after yielding for all samples due to the limitation of ductility of ultrafine-grained Cu, and the uniform ductility of the ECAP ultrafine-grained Cu is negligible. Klein et al. [14] explained the size effect on the fracture strain on the basis of different textures, but the influence of sample thickness on the uniform ductility is not very clear.

In addition, there are some other reasons why size effects occur. For example, sometimes, the grains seem too big compared to the small sample thickness and the material response is suggested to be dominated by the size and orientation of individual grains located in the deformed area [15]. In addition, the influence of surface defects (e.g. roughness) on the mechanical behavior will become more significant with decreasing sample thickness [13].

To date, the dependence of sample thickness on the flow stress of face-centered cubic materials has been investigated by both experimental and simulation studies. However, there is limited information available on

\* Corresponding author. Tel.: +86 24 23971939; e-mail: [llu@imr.ac.cn](mailto:llu@imr.ac.cn)

the uniform tensile ductility and work-hardening behavior of non-standard miniature metal samples. In this paper, the dependence of sample thickness effects on the tensile behavior, including yield strength, tensile strength, ductility and work hardening, of pure Cu with different grain sizes were investigated. Possible mechanistic origins of the observations are discussed.

A well-annealed coarse-grained Cu (CG Cu) sample prepared by means of electron beam melting and a fine-grained Cu (FG Cu) processed by friction stir processing (FSP) on a gantry friction stir welding machine were selected. Chemical analysis indicates that the purity of CG Cu and FG Cu are better than 99.99%. Scanning electron microscopy (SEM) observation with a Nova Nano 430 indicates that both CG Cu and FG Cu consist of equiaxed grains in three dimensions. The average grain size is about 82  $\mu\text{m}$  for CG Cu and 13  $\mu\text{m}$  for FG Cu.

The tensile sample was in a dog-bone shape with a gage length of 4 mm and a width of 2 mm. The sample thickness of the tested Cu samples varied from 100  $\mu\text{m}$  to 2 mm for CG Cu and to 0.5 mm for FG Cu to identify the dependence of thickness on the tension properties. All sheet samples were polished using SiC paper, following by chemically polishing to minimize the surface defects. Uniaxial tensile tests were performed on a Tytron 5848 microforce testing system with a strain rate of  $6 \times 10^{-3} \text{ s}^{-1}$  at room temperature. A contactless MTS LX300 laser extensometer (Eden Prairie, MN, USA) was used to calibrate and measure the sample strain upon loading. Laser scanning confocal microscopy (LSCM; LEXT OLS4000) was used to characterize the three-dimensional (3-D) surface topography of Cu samples after tensile tests.

An optical measurement system (ARAMIS, GOM mbH) was coupled with the tensile test machine to measure the local strain distribution on the front faces of the tension samples. The system consists of two high-resolution CCD cameras and an external controller which records the force data from the tensile test machine. The CCD cameras record images of the tension test specimen at every specified time interval [16]. The sample surface was painted with a random white and black dot pattern for recognizing the position and shape. The system divides the picture into many small squares, called facets, and calculates the local displacement of the facets. The local accuracy of strain deformation is up to 0.01%.

The tensile engineering stress-strain curves of CG and FG Cu samples with different thicknesses are shown in Figure 1a and b, respectively. It is clear that there is no obvious change in the yield stress ( $\sigma_y$ ) of Cu samples with decreasing sample thickness ( $t$ ). The elastic deformation stages of both Cu samples with different sample thicknesses are almost overlapped. The yield stress of CG Cu is around 50 MPa, which is consistent with the data reported in the literature [17]. However, there is a significant difference in the plastic deformation stages: a greatly improved tensile ultimate strength, uniform ductility as well as work hardening are observed in both Cu samples with increasing  $t$ . For example, there is no significant change in the ultimate tensile stress and ductility for CG Cu when  $t$  decreases from 1.0 to 0.5 mm, but a sudden reduction in ductility and tensile strength

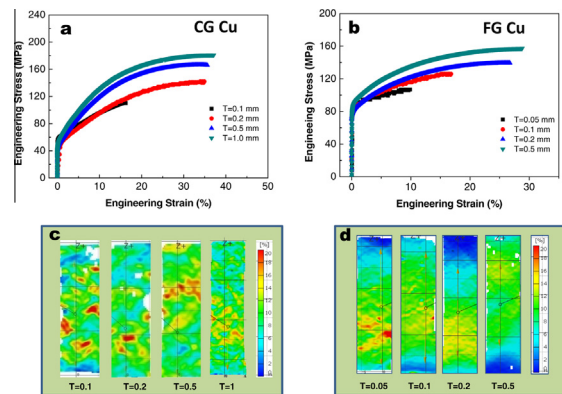


**Figure 1.** Tension engineering stress-strain curves of CG Cu (a) and FG Cu (b) samples with different thicknesses. The comparison of plastic strain distribution in gauge length for CG Cu (c) and FG Cu (d) samples at a fixed stain of 10% by means of ARAMIS. The gradient colors of the scale represent different local strains on the gauge surface.

was observed in CG Cu with  $t = 0.2$  mm. A similar thickness effect is also observed in FG Cu samples: the ultimate tensile strength decreased from 157 to 107 MPa and the tensile ductility from 24% to 10% when the sample thickness decreased from 0.5 to 0.05 mm.

Snapshots of the plastic strain distributions of the gauge surface of CG Cu and FG Cu samples are shown in Figure 1c and d, which are extracted from the ARAMIS movie recorders at a constant strain of 10%. The plastic strains in the gauge length are very inhomogeneous in the CG samples. The strain localization is more concentrated in the thinner CG Cu samples, as localized plastic strains  $>15\%$  (marked in red) are frequently seen in CG Cu  $\leq 0.1$  mm thick. Generally, more homogeneous plastic deformation was seen in the FG Cu samples than in the CG Cu samples. Almost no strain localization is detected in the gauge length of FG Cu with  $t \geq 0.5$  mm.

The influence of sample thickness on the tensile properties of both CG and FG Cu, including the yield strength, ultimate tensile strength, uniform strain and work-hardening coefficient, are summarized in Figure 2. In order to normalize the grain size effect, the ratio of specimen thickness to grain size ( $t/d$ ) is also considered as the  $x$ -axis in Figure 2. Clearly, the yield strength is insensitive to the sample thickness, while the ultimate

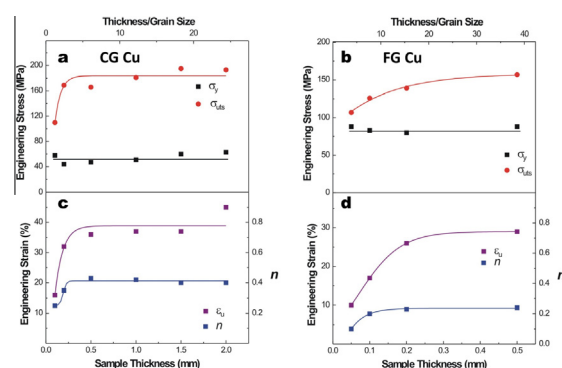


**Figure 2.** Sample thickness effect on the tensile yield strength/tensile strength, uniform strain and work-hardening coefficient of CG Cu (a and c) and FG Cu (b and d).

strength increases gradually with increasing sample thickness, and then reaches a saturated stage when  $t/d$  is larger than a critical value, which is similar to the behavior found in Cu and Cu–Al alloys [10,18]. Moreover, the critical  $t/d$  value for the uniform strain and work hardening is also observed in Figure 2c and d, where saturated strain and work-hardening coefficient are also achieved at the same critical  $t/d$ . Here the work-hardening coefficient ( $n$ ) is computed from the uniform plastic deformation stages in Figure 1a and b according to the Hollomon–Ludwik power law [19,20]. The critical  $t$  is  $\sim 0.5$  mm (or  $t/d = 6$ ) for CG Cu, and  $\sim 0.2$  mm (or  $t/d = 18$ ) for FG Cu. This means that the critical value depends not only on the sample thickness, but also on the average grain size ( $d$ ) of the sample. A larger critical thickness and a smaller ratio of  $t/d$  are expected for the sample with larger average grain size. It is noteworthy that only above the critical  $t/d$ , the value of uniform elongation ( $\varepsilon_u$ ) is roughly equivalent to the value of the work-hardening exponent ( $n$ ), as predicted by the Hollomon law [20].

Detailed plane- and top-view SEM observations are performed on the CG and FG Cu samples after tensile tests to analyze the failure processes, as shown in Figure 3. A general phenomenon can be found that the thinner Cu samples ( $t = 0.2$  mm) prefer to sustain a pure shear failure with typical knife edge fracture topography (Fig. 3a1,a2 and c1,c2), while the thicker Cu samples ( $t = 1.5$  mm) exhibit normal tensile failure with significant necking in both thickness and width directions (Fig. 3b1,b2 and d1,d2). A few dimples are observed in the top-view SEM images of CG and FG Cu samples with thinner thickness ( $t = 0.2$  mm), but some fine tension dimples and voids are observed in the fracture surface of CG and FG Cu of greater thickness ( $t = 1.5$  mm), as shown in Figure 3a3,b3 and c3,d3. It is suggested that the failure mode changes gradually from pure shear failure to a normal tensile failure for both Cu samples with increasing sample thickness.

Surface morphology evolution during plastic deformation, especially roughness, will reduce tensile ability by premature failure as well. Such an influence will become more significant with decreasing sample thickness [13]. In the present study, the tension specimens are polished carefully in order to minimize the original surface defects; however, during the tension tests, the free surface of the specimen becomes rough with increasing plastic strain.

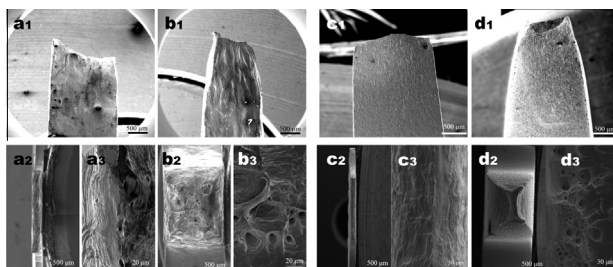


**Figure 3.** Plane-view and top-view SEM observations on the surfaces of Cu after tensile tests: (a1–a3)  $t = 0.2$  mm for CG Cu; (b1–b3)  $t = 1.5$  mm for CG Cu; (c1–c3)  $t = 0.2$  mm for FG Cu; (d1–d3)  $t = 1.5$  mm for FG Cu. Images a3–d3 are high-magnification images of a2–d2, respectively.

Wouters et al. [21,22] also found a linear relation between root-mean-square roughness and both strain and grain size, which is explained as arising from orientation differences between neighboring grains and depends on the available number of slip systems in the materials. The softer grains, usually with high Schmid factor, will deform more than harder grains and cause an inhomogeneous thinning of the material during tensile deformation and local variation in surface height (roughness).

The surface morphologies of CG and FG Cu samples (with  $t = 0.5$  mm) at a tensile strain of  $\sim 30\%$  are shown in Figure 4. Compared with the flattened surface with negligible surface roughness before tensile tests, rough surfaces can be clearly seen after deformation. The surface roughness fluctuated within almost  $100\ \mu\text{m}$  for CG Cu with an average surface roughness of  $11.8\ \mu\text{m}$ , which was obtained from the arithmetic average of the absolute values of the roughness profiles from Figure 4. The average surface roughness of FG Cu is  $1.5\ \mu\text{m}$ , smaller than that of CG Cu. When the ratio of additional surface roughness to sample thickness is big enough, the influence of the additional roughness on the tensile behavior has to be considered. In order to quantitatively understand the surface roughness effect on the plastic deformation, we introduce the surface roughness ( $R$ ) to correct the relationship between  $n$  and  $\varepsilon_u$ . Because of  $R$ , the real cross-section area ( $A'$ ) of sample is smaller than the theoretical value ( $A$ ), as assumed:

$$A' = A \left(1 - \frac{2R}{t}\right) = A\eta. \quad (1)$$

The relationship between  $n$  and  $\varepsilon_u$  can then be expressed by:

$$\frac{d\sigma}{d\varepsilon} = \sigma \left(1 - \frac{d\eta}{\eta d\varepsilon}\right) \quad (2)$$

$$n = \varepsilon_u \left[1 + \frac{2dR}{(t - 2R)d\varepsilon}\right]. \quad (3)$$

If there is no additional surface roughness or the additional surface roughness is negligible compared with the sample thickness, where  $t \gg R$ , then  $n$  is approximately equal to  $\varepsilon_u$ . This is the ideal case for the sufficiently thick samples, in which the uniform elongation ( $\varepsilon_u$ ) is numerically equal to the work-hardening coefficient ( $n$ ) as predicted by Hollomon's law [19]. However, for thin specimens with thickness less than the critical  $t$ , when the surface roughness  $2R$  is comparable to the thickness  $t$ , it is obvious that the measured  $\varepsilon_u$  would be smaller than  $n$  due to the effects of additional surface

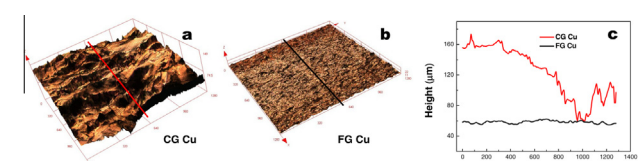


**Figure 4.** The 3-D surface morphology by LSCM of CG (a) and FG (b) with  $t = 0.5$  mm, at about  $30\%$  engineering strain. Image (c) shows the primary profiles along lines 1 and 2 for CG and FG Cu samples, respectively.

roughness. This is consistent with the experimental results that a smaller  $\varepsilon_u$  (0.16) is detected in the CG Cu with  $t = 0.1$  mm, compared with the  $n$  value (0.25).

For polycrystalline metals, dislocation slip in the grains is one of the dominant plastic deformation mechanisms, in which dislocation can either be blocked by the grain boundary or glide out of the surface and leaving behind a surface step [23]. All grains in the interior of the samples deform homogeneously, but the grains close to the sample surface are less constrained by the surrounding grains, and less dislocation can accumulate in surface grains, as compared to interior grains. An increased number of surface grains means lower work hardening and lower flow stress. As indicated by Wouters et al. [21,22], the surface roughness of the deformed sample is determined by multiple layers of grains rather than just by the surface grains. In particular, it should be noted that both the top surface and the subsurface grains influence the roughness and should be responsible for the degradation of tensile properties. The number of grain layers across “surface layer” decreases with increasing grain size [10], which can explain why the critical value of  $t/d$  of FG Cu is bigger than that of CG Cu in Figure 2.

In this study, the sample thickness is in the range of hundreds of micrometers to a few millimeters, most of which still meet the definition of macro-size samples and the specimens are a few grains thick. When  $t/d$  is larger than the critical value mentioned above, the sample is sufficiently thick that abundant grain boundaries can trap the dislocation and act as sources to produce new ones: no obvious sample size effect is then found. When  $t/d$  is below the critical value, the effect of grains in the surface layer becomes dominant. These grains are less constrained because the surface is a softer obstacle to blocking dislocations compared to the grain boundaries. Therefore, the strength and elongation decrease with decreasing  $t/d$  in this regime, i.e. “smaller is weaker”. However, if  $t/d$  further decreases, that means only a few or no grain boundaries are present across the specimen thickness, as found in nanopillars [24], nanowires [25] and thin films [26], and a strong size effect of “smaller is stronger” is prominent. Greer and Hosson [27] presented a 3-D plot which revealed the combined effects of diameter and grain size on the strength of pure Ni and Ni alloy with a sample diameter on the nanoscale. Several interesting aspects of size-dependence deformation, similar to the present study, were revealed and a phenomenon of “smaller is weaker” was also observed in pillar samples with a small range of diameter of 200–300 nm under nanoindentation. In this case, accumulation of dislocations is limited because once the dislocations have been generated, they can slip out of the specimen easily. The scarcity of grain boundaries also limits the sources of dislocations, and the strength would strongly depend on specimen size, which is another story and beyond the scope of this paper.

In summary, we have demonstrated that an apparent sample thickness effect exists for tensile strength, uniform ductility and work hardening of Cu with different grain sizes. The tensile strength, uniform strain and work-hardening coefficient of Cu samples with different grain sizes decrease as the ratio of specimen thickness/grain size ( $t/d$ ) decreases below a critical value. The critical value of

$t/d$  depends on the grain size as well: the larger the grain size, the smaller the critical value. The mechanical properties of metals are mainly governed by competition between the dislocation activities in the interior and surface grains, while the volume fraction of surface grains is closely related to the sample thickness.

The authors acknowledge the National Basic Research Program of China 973 Program (2012CB932202), the financial support from the National Science Foundation of China (Grant Nos. 51071153, 50911130230). L.L. thanks the financial support of the “Hundred of Talents Project” by the Chinese Academy of Sciences. The authors are grateful to Prof. Z.Y. Ma for providing the FSP Cu samples.

- [1] E.O. Hall, Proc. Phys. Soc. London Ser. B 64 (1951) 747–753.
- [2] N.J. Petch, J. Iron Steel Inst. 174 (1953) 25–28.
- [3] F. Dalla Torre, H. Van Swygenhoven, M. Victoria, Acta Mater. 50 (2002) 3957–3970.
- [4] Y.M. Wang, E. Ma, Appl. Phys. Lett. 83 (2003) 3165–3167.
- [5] R.P. Reed, A.F. Clark, Materials at low temperatures, in: American Society for Metals, Materials Park, OH, 1983.
- [6] <<http://www.astm.org>>.
- [7] M. Dao, L. Lu, R.J. Asaro, J.T.M. De Hosson, E. Ma, Acta Mater. 55 (2007) 4041–4065.
- [8] H. Gleiter, Prog. Mater. Sci. 33 (1989) 223–315.
- [9] M.A. Meyers, A. Mishra, D.J. Benson, Prog. Mater. Sci. 51 (2006) 427–556.
- [10] S. Miyazaki, K. Shibata, H. Fujita, Acta Metall. 27 (1979) 855–862.
- [11] T. Fulop, W.A.M. Brekelmans, M.G.D. Geers, J. Mater. Process. Technol. 174 (2006) 233–238.
- [12] T.A. Kals, R. Eckstein, J. Mater. Process. Technol. 103 (2000) 95–101.
- [13] Y.H. Zhao, Y.Z. Guo, Q. Wei, A.M. Dangelewicz, Y.T. Zhu, T.G. Langdon, Y.Z. Zhou, E.J. Lavernia, C. Xu, Scr. Mater. 59 (2008) 627–630.
- [14] M. Klein, A. Hadrboletz, B. Weiss, G. Khatibi, Mater. Sci. Eng. A-Struct. Mater. Prop. Microstruct. Process. 319–321 (2001) 924–928.
- [15] U. Engel, R. Eckstein, J. Mater. Process. Technol. 125 (2002) 35–44.
- [16] H. Hoffmann, S. Hong, CIRP Ann-Manuf. Technol. 55 (2006) 263–266.
- [17] R.P. Carreker Jr, W.R. Hibbard Jr, Acta Metall. 1 (1953) 654–663.
- [18] S. Miyazaki, H. Fujita, Trans. Jpn. Inst. Met. 19 (1978) 439–444.
- [19] J.H. Hollomon, Trans. AIME 162 (1945) 268–290.
- [20] P. Ludwik, Elemente der technologischen mechanik, Springer-Verlag, Berlin, 1909.
- [21] O. Wouters, W.P. Vellinga, R. Van Tijum, J.T.M. De Hosson, Acta Mater. 54 (2006) 2813–2821.
- [22] O. Wouters, W.P. Vellinga, R. Van Tijum, J.T.M. De Hosson, Acta Mater. 53 (2005) 4043–4050.
- [23] M.G.D. Geers, W.A.M. Brekelmans, P.J.M. Janssen, Int. J. Solids Struct. 43 (2006) 7304–7321.
- [24] M.D. Uchic, D.M. Dimiduk, J.N. Florando, W.D. Nix, Science 305 (2004) 986–989.
- [25] G. Richter, K. Hillerich, D.S. Gianola, R. Monig, O. Kraft, C.A. Volkert, Nano Lett. 9 (2009) 3048–3052.
- [26] E. Arzt, Acta Mater. 46 (1998) 5611–5626.
- [27] J.R. Greer, J.T.M. De Hosson, Prog. Mater. Sci. 56 (2011) 654–724.